Penerbit Akademia Baru

CFD Letters

Journal homepage: www.akademiabaru.com/cfdl.html
ISSN: 2180-1363

Numerical Modelling for Natural Oil Convection of Non-Guided Winding Cooling Arrangement

Open Access

Zulkifli Ibrahim[1,2,*], Mohd Zainal Abidin Ab Kadir[1,3], Norhafiz Azis[1], Jasronita Jasni[1], Mahdi Izadi[1], Muhammad Hakirin Roslan[4]

[1] Centre for Electromagnetic and Lightning Protection Research (CELP), Advanced Lightning and Power Energy Research (ALPER), Universiti Putra Malaysia, 43400 Serdang, Selangor, Malaysia
[2] Faculty of Electrical and Electronic Engineering Technology, Kampus Teknologi, Universiti Teknikal Malaysia Melaka, Hang Tuah Jaya, 76100 Durian Tunggal, Melaka, Malaysia
[3] Institute of Power Engineering (IPE), Universiti Tenaga Nasional, 43000 Kajang, Selangor, Malaysia
[4] Faculty of Engineering, Universiti Pertahanan Nasional Malaysia, Kem Sg Besi, 57000 Kuala Lumpur, Malaysia

ARTICLE INFO

Article history:
Received 20 February 2020
Received in revised form 18 April 2020
Accepted 22 April 2020
Available online 30 April 2020

Keywords:
Hot-spot temperature; natural oil convection; non-guided oil flow; CFD; conjugate heat transfer

ABSTRACT

The hot-spot temperature is a key parameter in transformer loading management. It plays a significant role in evaluating transformer winding thermal performances, as well as in the determination of winding insulation's loss of life. A simplified winding thermal model has been developed based on the presented methodology in favour to reduce real-world model complexity. A conjugate heat transfer has been approached to solve the cooling effects of natural oil convection. Results show a good agreement with only 3.1% percentage difference for the average winding temperature between the newly developed winding model and manufacturer factory-end test report. The plotted graphs of oil flow and thermal distributions showed a unique relation between localised hot-spot temperature and oil flow patterns. The hottest temperature and its location are well pronounced with the inclusion of eddy current loss distribution within winding height. The proposed methodology can be used to investigate the oil cooling scheme of transformer winding and allows the manufacturers to optimise their thermal design.

1. Introduction

Power transformer plays a vital role in transporting electrical energy from one end to another. It is also the most expensive single piece of an electrical component in the entire electrical system network. The malfunction of power transformer will be a catastrophe in both technical and financial aspects. One of the essential criteria in monitoring the health of transformer operation is the hot-spot temperature, which is directly proportional to the loading condition and the rate of degradation

* *Corresponding author.*
E-mail address: zulib.utem@gmail.com (Zulkifli Ibrahim)

https://doi.org/10.37934/cfdl.12.4.5467

of insulation materials, as reported by Kassi *et al.,* [1]. CIGRE Working Group A2.24 [2] and CIGRE Task Force [3] reported that loading of transformer beyond nominal rating will increase the generation of heat, consequently, increases the winding hot-spot temperature above the critical value that is 98°C for normal and 110°C for thermally-upgraded insulation papers. These critical temperature limits are derived at which the rate of insulation paper (cellulose-based material) degradation is at unity, as explained in both international standards IEC 60076-7 [4] and IEEE Std C57.91-1995 [5]. Hence, managing the hot-spot temperature is crucial to keep the operating temperature below the critical limits that could prevent premature ageing of this cellulose-based insulation material. In a collective maintenance report prepared by CIGRE Working Group A2.37 [6], the oil-immersed transformer has an active life between 25 and 40 years when operating continuously at normal designed-rate of winding insulation degradation.

Two types of winding cooling arrangements, namely guided oil flow (GOF) and non-guided oil flow (NGOF), are widely used in transformer winding cooling design. The GOF type is typically for high power transformer while the NGOF is for medium power transformers. Apart from being electrical insulation, the oil inside the transformer also acts as a cooling medium which circulates through windings (heat source) and radiators (heat sink). This circulation of oil is established by the natural convection phenomena, where the oil flow velocity and pattern are driven by the buoyancy force due to the change in oil temperature and density as found in the Lecuna *et al.,* [7]'s article. As the oil flow behaviors (velocity and pattern) in the natural oil convection are difficult to control, it is crucial to size the vertical and radial oil ducts precisely. In this case, the winding hot-spot temperature would be lower than the critical limit.

In the earlier of CFD thermal model for transformer winding studies, there were found very few researchers conducted research on the NGOF transformer winding. For instance, from the past studies, more than 70% of research works performed an extensive study on the GOF winding type (based on 54 most related paper journals). The popularity of GOF research over NGOF is due to the reason that the calculation of the GOF can be based on the theoretical explanation which uses thermal-hydraulic network model (THNM), which can be found in the Weinläder *et al.,* [8]'s article. The oil flow and temperature distribution of GOF can be solved independently for every oil duct; thus, the hot-spot temperature of disc winding can be known and located. On the other hand, Mufuta *et al.,* [9] reported that the formulation and calculation of NGOF are empirically derived. As such, it is not possible to justify the flow pattern and the hot-spot criteria without a physical test.

Despite that, there are drawbacks for GOF type. The major drawback is the temperature gradient between the top and bottom winding could be too big which requires a complex overall cooling design scheme. Besides, manufacturing time for the GOF winding is much longer than NGOF due to carefully fix the oil guide washer or block in order to avoid any occurrence of oil leakage which could lead to major winding failure as studied by Paramane *et al.,* [10].

Due to the lack of research in the NGOF, this present work focuses on the development of CFD with finite element discretization of 2D approximation for full NGOF winding with an intermediate axial cooling duct. This study aims to develop a simplified 2D axisymmetric FE-CFD (2D FE-CFD) approximation to replace the complex of real-world three-dimensional (3D) geometry. The CFD method was approached in order to obtain the pattern of fluid flow and thermal distribution within a complete NGOF type of a low voltage winding, 30MVA medium power transformer. One of the goals in using the CFD approximation is to understand the physical behaviors on thermal distribution, which arise in the event of fluid flows around, on the surfaces and inside the winding.

2. Methodology

The adaptation of a 2D FE-CFD model to replace the real-world 3D geometry can be realized in a commercial finite element based CFD software, COMSOL Multiphysics. A general work-frame of methodology structure in developing 2D FE-CFD winding model is illustrated in Figure 1. As can be seen from Figure 1, two types of data must be made available, namely the temperature rise test report and the winding design data. The winding design data was used to develop the physical geometry of the model, while the data from the test report was used for both setting-up the initial condition of computer simulation and model validation. It is also clear that the parameter of interest to validate the model is the average winding temperature.

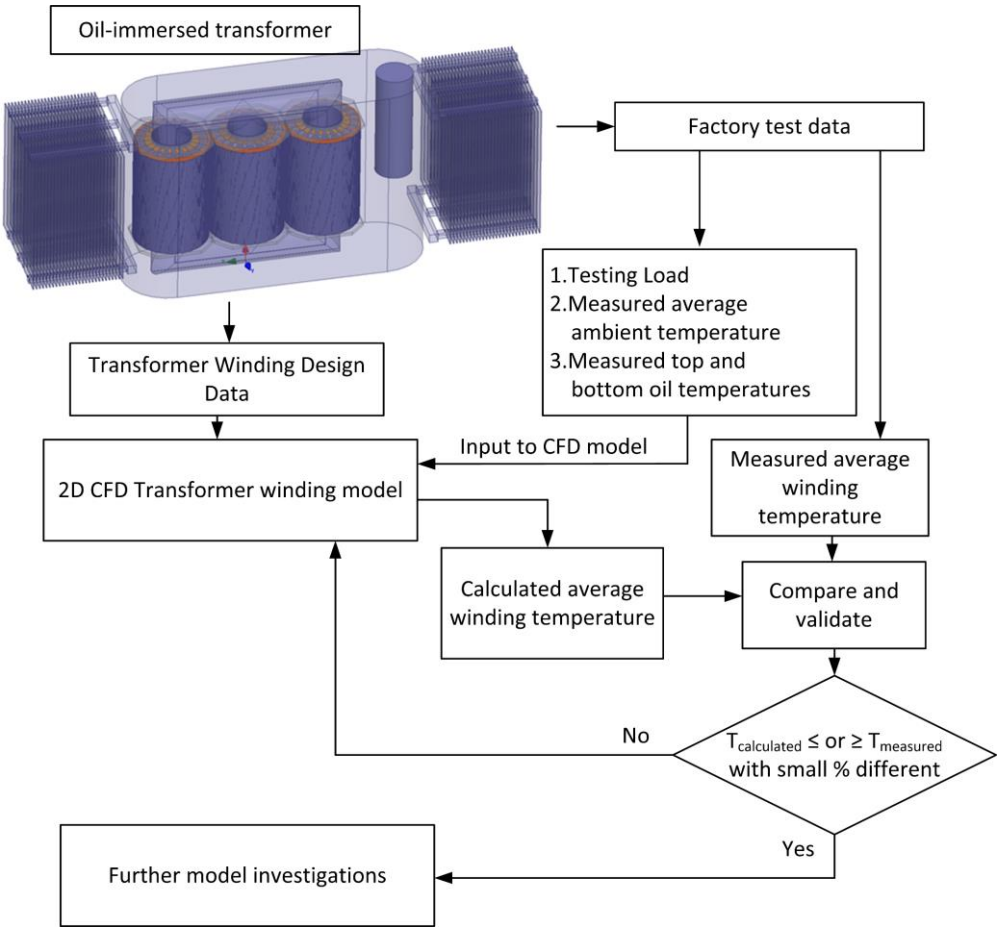

Fig. 1. Methodology chart

2.1 Model Geometry

A commercial unit three-phase 30MVA 33/11kV medium power transformer with ONAN/ONAF cooling modes with the rated short circuit impedance of 10% was selected as the studied transformer. Figure 2 shows the derivation of two-dimensional winding model approximation. The detailed of 11 kV low voltage winding is shown in Figure 3. The overall winding height,H is 1540 mm consists of 94 discs with each disc has 25 parallel conductors. Each disc is separated by 4 mm axial spacer (Ax) to form radial/horizontal cooling ducts. The height of cooling band, b is 5 mm placed after the 12th strand (counted from left to right) to form an intermediate cooling duct. The width of the outer (OD) and inner (ID) cooling ducts are 12 mm and 9 mm respectively. The individual copper strand sizes of 13 (h) mm x 2.1 (w) mm covered by 0.65 mm Kraft paper (t).

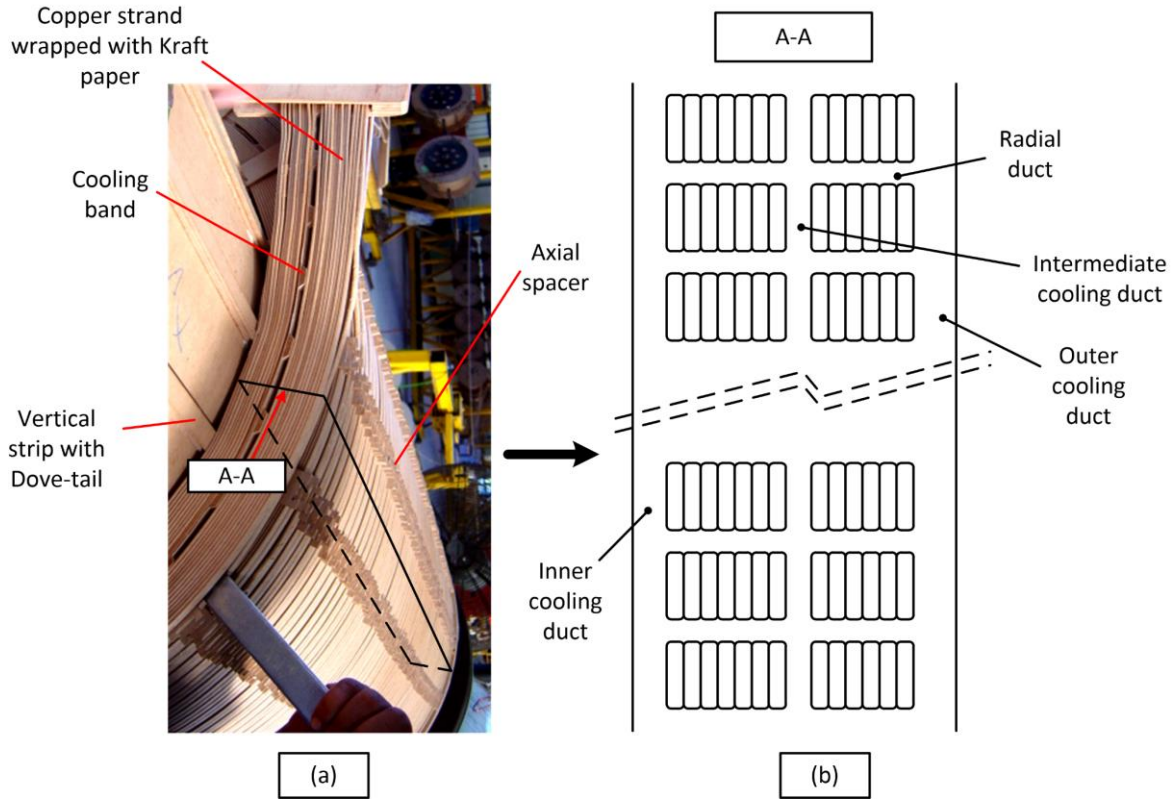

Fig. 2. Derivation of 2D axisymmetric winding geometry from A-A view cut-out, (a) actual disc winding and (b) 2D detailed model

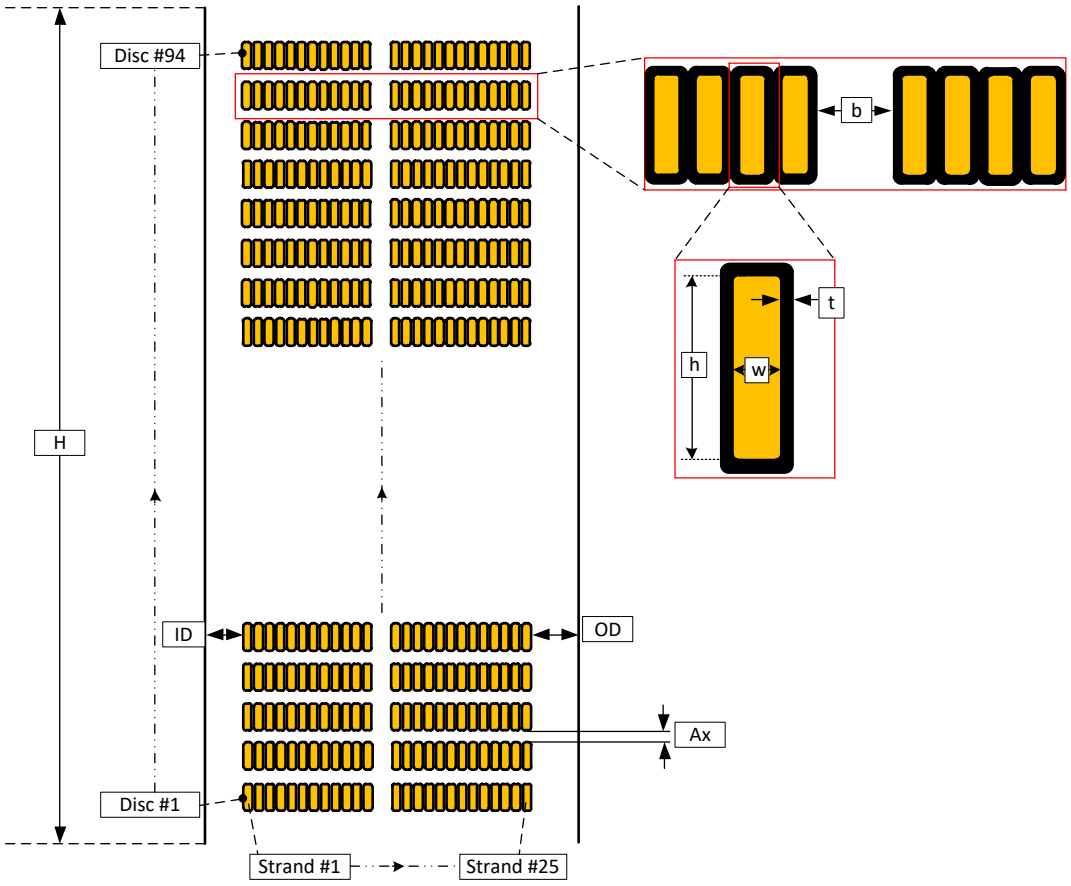

Fig. 3. 2D axisymmetric low voltage winding details

2.2 Material Properties

According to Ghani *et al.,* [11], the transformer oil is derived from petroleum mineral oil. This oil was configured as the only temperature-dependent material inside transformer main tank. The thermal properties of this oil are similar to the one used in the Torriano *et al.,* [12,13]'s thermal model studies, can be written as

$$\rho_f = 884.2 - 0.721 \cdot T \tag{1}$$

$$C_{Pf} = 1807 + 4.5 \cdot T \tag{2}$$

$$k_f = 0.115 - 4.4414 \cdot 10^{-5} \cdot T \tag{3}$$

$$loglog(v_f + 0.7) = A - (B \times log(T + 273)) \tag{4}$$

Two solid materials are used to construct the transformer winding, both of which are copper conductor and insulation paper. The following thermal properties of solid materials were also can be found in the El Wakil *et al.,* [14]'s article.

$$\rho_c = 8700$$

$$\rho_p = 930$$

$$C_{Pc} = 385$$

$$C_{Pp} = 1340$$

$$k_c = 400$$

$$k_p = 0.19$$

where ρ is the oil density (kg m^{-3}), C_P is the oil specific heat capacity at constant pressure (J kg^{-1} K^{-1}), k is the oil thermal conductivity (W m^{-1} K^{-1}), v is the kinematic viscosity of oil (m s^{-2}) and T is the absolute temperature in ºC. Constant A and B are 10.3062 and 4.1431, respectively. The subscripts letters f, c and p in the materials property's expressions are for transformer oil, copper conductor and insulation paper, respectively.

2.3 Boundary Conditions

Boundary conditions for system computation are shown in Figure 4. At the inlet, an open boundary condition is set with normal stress equals to zero. This configuration was recommended in the COMSOL CFD User's guide [15] in order to allow the oil flows in or out from the system via this boundary freely. The temperature at this boundary, T0 is 66.7°C. At the outlet, the pressure is set to zero with suppress backflow to prevent the oil from entering the domain through this boundary and assigned for convection dominated heat transfer. Both inner and outer cylindrical pressboards are specified as thermally insulated, which means no heat transfers occur across the boundary.

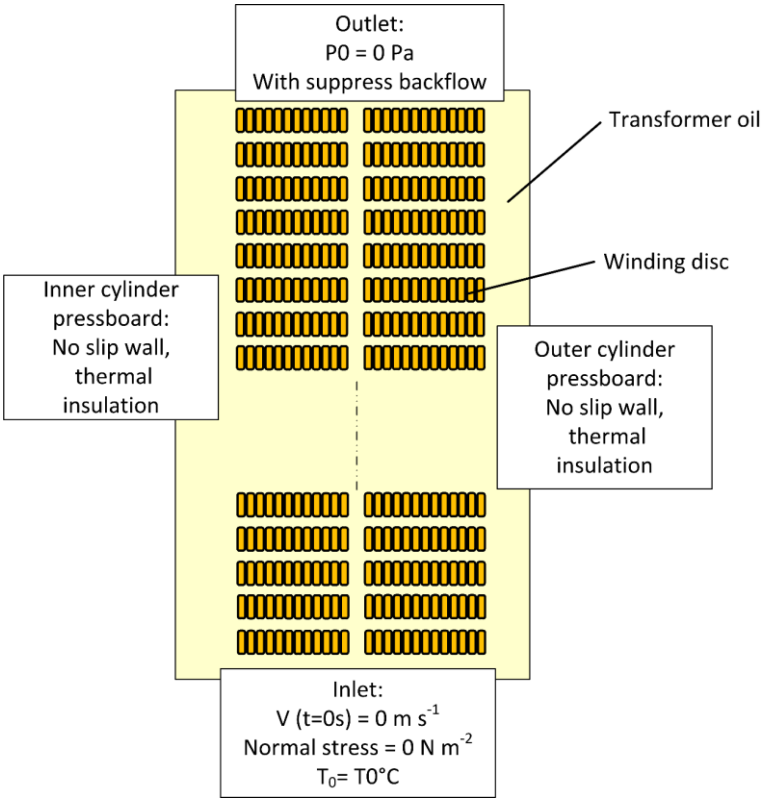

Fig. 4. Boundary conditions

2.4 Heat Source Distributions

Total winding losses are non-uniformly distributed along with the winding height due to the variation of the flux density penetration into the discs. Practically, the top-most and bottom-most discs have experienced a huge amount of flux density; thus, in turn, they have the highest induced eddy current. Wijaya *et al.,* [16] describes the total winding losses (P_{TL}) can be categorized into a direct current loss (P_{DC}) and eddy current loss (P_{EC}) as the following

$$P_{TL} = P_{DC} + P_{EC} \tag{5}$$

The direct current loss is defined as

$$P_{DC} = \frac{J^2 \times m}{\sigma \rho} \tag{6}$$

where J is the current density (A m^{-2}), m is the copper mass (kg), σ is the conductivity of copper (S m^{-1}) and ρ is the copper density (kg m^{-3}). The eddy current loss is expressed by

$$P_{EC} \cong \frac{\sigma \cdot \pi^2 \cdot h^2 \cdot f^2 \cdot B^2}{3} \tag{7}$$

where h is the conductor width in the direction of the magnetic flux density, B and f are the magnetic flux density (Wb m^{-2}) and frequency (Hz) respectively. From the equations above, the calculated total winding losses are 16525 W and non-uniformly distributed on every disc as can be seen in Figure 5. The losses distribution in Figure 6 is the heat source for the winding model. The contour plot of the heat source distribution (W m^3) on each disc for the 94 full discs winding model is shown in Figure 6.

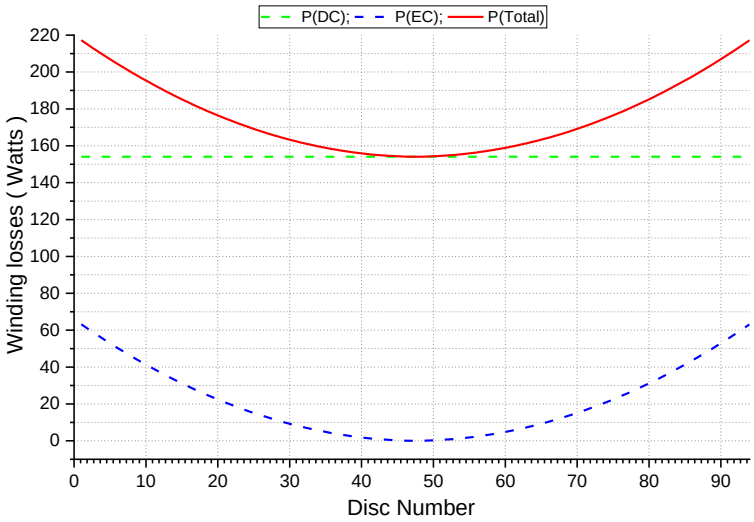

Fig. 5. Winding total losses distribution

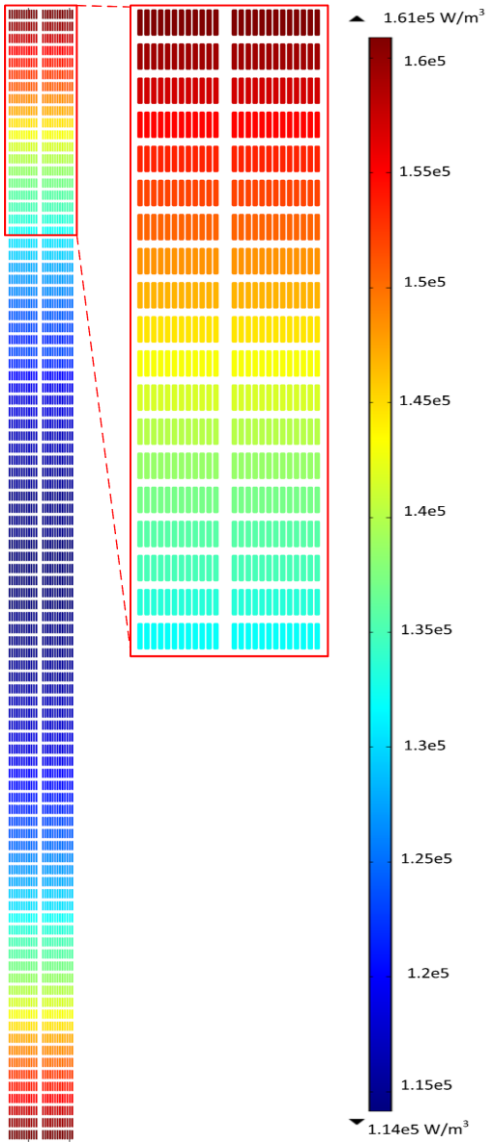

Fig. 6. Full winding non-uniform heat loss distribution due to eddy current losses in W/m^3

2.5 Governing Equation

A conjugate heat transfer (CHT) was applied to solve strong coupling between heat transfer and fluid dynamic problems. This approach was also performed by Chereches *et al.,* [17]. Finite element method-based COMSOL Multiphysics software was adopted to solve Navier-Stokes equations for weakly compressible fluid, continuity equation and energy equation. Time-dependent solver with absolute tolerance 5×10^{-4} and (backward differentiation formula) BDF time-stepping method were utilized to solve these equations. Free time step was set (automatic chose the time steps freely). The time-dependent solver node has two sub-nodes solvers, Fully coupled and Iterative. The Fully coupled used iterative linear solver which applied constant (Newton) damping factor 0.9 for nonlinear method of termination. The iterative used GMRES solver with 50 number of iterations. These equations were solved directly without considering Boussinesq approximation as described in COMSOL CFD User's Guide [18] which can be written as the following

Conservation of momentum equation

$$\rho \frac{\partial u}{\partial t} + \rho(u \cdot \nabla)u = \nabla \cdot \left[-\rho I + \mu(\nabla u + (\nabla u)^T) - \frac{2}{3}\mu(\nabla \cdot u)I\right] + F \tag{8}$$

Continuity equation for the conservation of mass

$$\frac{\partial \rho}{\partial t} + \nabla \cdot (\rho u) = 0 \tag{9}$$

and conservation of energy equation

$$\rho C_p \frac{\partial T}{\partial t} + \rho C_p u \cdot \nabla T = \nabla \cdot (k \nabla T) + Q \tag{10}$$

where u is the velocity vector (m s^{-1}), μ is the dynamic viscosity (kg m^{-1} s^{-1}), F is the volume force (N m^{-3}) and Q is the heat source (W m^{-3}). In order to incorporate the natural convection of oil, the buoyancy force can be defined as the volume force, $F = g * (\rho - \rho_{ref})$, where g is the gravitational acceleration (m s^{-2}) and ρ_{ref} is the reference oil density at the initial temperature of the system.

In Chereches *et al.,* [17]'s previous works, the flow condition was characterized by three dimensionless parameters as the following

Reynolds number

$$R_e = \frac{\rho U_b L}{\mu}, \tag{11}$$

Grashof number

$$G_r = \frac{g \beta \Delta T L^3}{v^2} \tag{12}$$

Prandtl number

$$P_r = \frac{v}{\alpha'} \tag{13}$$

where U_b is the oil bulk velocity (m s^{-1}), L is the characteristic length (m), β is the thermal expansion coefficient (K^{-1}) and α is the thermal diffusivity (m^2 s).

Reynolds number used to characterize the fluid flow regime whether laminar, transition or turbulence. In the heat transfer textbook by Lienhard IV and Lienhard V [19], the critical value of R_e in order to keep the fluid flow in fully-developed laminar flow regime is 2100. From literature studies, the typical value of R_e for natural convection of oil in NGOF type is approximately 25 ~ 100, as such, the oil flow near to the boundary/wall is always in the laminar regime as reported by Skillen *et al.,* [20] and Kranenborg *et al.,* [21]. The G_r determines the influence of buoyancy force in transformer oil flow. It measures the ratio of buoyancy forces to viscous forces. Usually, the convective boundary layer is laminar when $G_r < 10^8$. The third parameter, P_r that measures the ratio of oil viscosity to the thermal diffusivity. This parameter shows the impact of oil viscosity on the thermal diffusivity. Generally, the P_r value is in the range of 40 to 400 for transformer mineral oil depending on temperature range and oil type, this high value of P_r shows that oil viscosity has a significant effect on thermal diffusivity as found in the Torriano *et al.,* [22]'s article and COMSOL CFD User's Guide [23]. Later, the flow of oil was distinguished between in forced and natural convection regime by the ratio of G_r/R_e^2 . The flow is said to be in forced convection if $G_r/R_e^2 \ll 1$ and in natural convection regime if $G_r/R_e^2 \gg 1$.

3. Results and Discussion

3.1 Mesh Independent Study and Model Validation

A hybrid mesh used in this CFD simulation consists of thin quadrilateral mesh type for the flow boundary layers and triangles for the rest of the fluid flow domain. As indicated in Table 1, mesh independency studies for the different sizes of mesh (Mesh 1 and Mesh 2) were conducted to ensure the accuracy of the solutions. The number of elements of Mesh 2 was increased by threefold from Mesh 1 (50% different number of elements is sufficient as recommended by the software user's manual [23]). It reveals that the accuracy of the solutions for the meshes has deviated slightly with percentage difference 1.7 % and 0.2 % for the average winding temperature (T_{WDG_AVE}) and the average duct oil temperature (T_{DUCT_AVE}) respectively. The T_{WDG_AVE} was determined by averaging the temperature values of all discs in the winding. The T_{DUCT_AVE} is calculated by averaging the oil temperature values in the entire oil domain. Due to less computational demands, Mesh 1 was chosen for the entire present CFD simulation works. To converge a solution, approximately 5 to 7 days solution run time is required for time-dependent solver based on the size of the model running on 24 cores of CPU and 128 GB RAM computer.

The model is validated by comparing the test data from factory-end temperature rise test report to the data obtained from 2D CFD simulation results. The only available measured data for comparison is the average winding temperature as tabulated in Table 2. As seen in Table 2, it worth mentioning that there have been relatively small differences between the simulation result of Mesh 1 and measured data with the percentage difference of 3.1%.

Table 1
Mesh independency analysis

Mesh	Mesh 1	Mesh 2
No. domain element	1 323 963	4 227 819
N_{de}/mm^2	9.40	30.01
T_{WDG_AVE}	77.59ºC	78.94 ºC
T_{DUCT_AVE}	71.84 ºC	71.96 ºC

Table 2
Model Validation

Parameter	CFD (Mesh 1)	Measured	Percentage difference %
T_{WDG_AVE}	77.59 ºC	80.04 ºC	3.1

3.2 Contour Plots of Thermal and Radial Component of Oil Flow Distributions

Figure 7 illustrates the thermal distribution for the full 94 discs of 11 kV low voltage winding model, 30 MVA medium power transformer. As seen, a small amount of temperature rises from bottom (oil inlet) to the top (oil exit) of the winding just by 5.5 K (72.2ºC - 66.7ºC). The small temperature gradient (top to bottom) is expected for NGOF with natural convection of oil. There are six spots of localised high temperatures developed in the winding where the hottest region is in the upper part of the winding but not at the top-most disc. The localised winding hot-spot developed at strand number 6 (counted from left to right) of disc number 93 as presented in Table 3. In this case, the calculated dimensionless parameters are 696, 1.25 x 10^7, 81 and 26 for $\mathrm{R_e}$, $\mathrm{G_r}$, $\mathrm{P_r}$ and $\mathrm{G_r/R_e^2}$ respectively.

Table 3
Winding hot-spot temperature and details information

Winding hottest temperature / ºC	Location	Adjacent radial oil velocity field / mm·s^{-1}	Mass flow rate at the inlet / kg·s^{-1}
96.7	Strand no.6 of disc 93	Top: 0.144 Bottom: -0.062	1.208

As can be depicted in Figures 8, the contour plots have been filtered out to show only radial oil flow with flow range + 1 mm/s (right-direction) to – 1 mm/s (left-direction). As can be seen, there are creations of zones where the oil circulates around the same position (eddies) or the oil is almost at rest (stagnant). These zones are marked by red circles (dotted line). This situation introduced a critical zone due to oil stagnant by which affected the efficiency of heat transfer from the heated oil to the ambient. To make it worse, these areas give rise to the adjacent disc temperature to an impulsive final value. In other words, these areas caused localised overheating which could place the winding hot-spot location. These flow characteristics are due to the interaction between velocity and pressure field as well as buoyancy force, where at a certain point the intensive heat absorbed by the oil in the horizontal channels is almost similar. As such, the pressure gradient between both junction end of the horizontal channels dropped. In that way, the retardation of collective oil flow occurs, and the inversion of its direction can be observed. There are three spots of critical zones found in the winding.

In oil natural cooled (ON) transformer, free convection of heat transfer occurs where the flow of oil is strongly patterned by the buoyancy force. The conduction of heat occurs between solid materials (conductor strands), the heat moves from the matters of more heat to matters of less heat by direct contact. It is interesting to note, the hot-spot is located at the centre of inner disc section (the 6th strand of disc 93). This can be explained by other strands has a much lower temperature due to its lack of neighbouring strands, consequently, has more free surface areas to dissipate heats (especially for end strands).

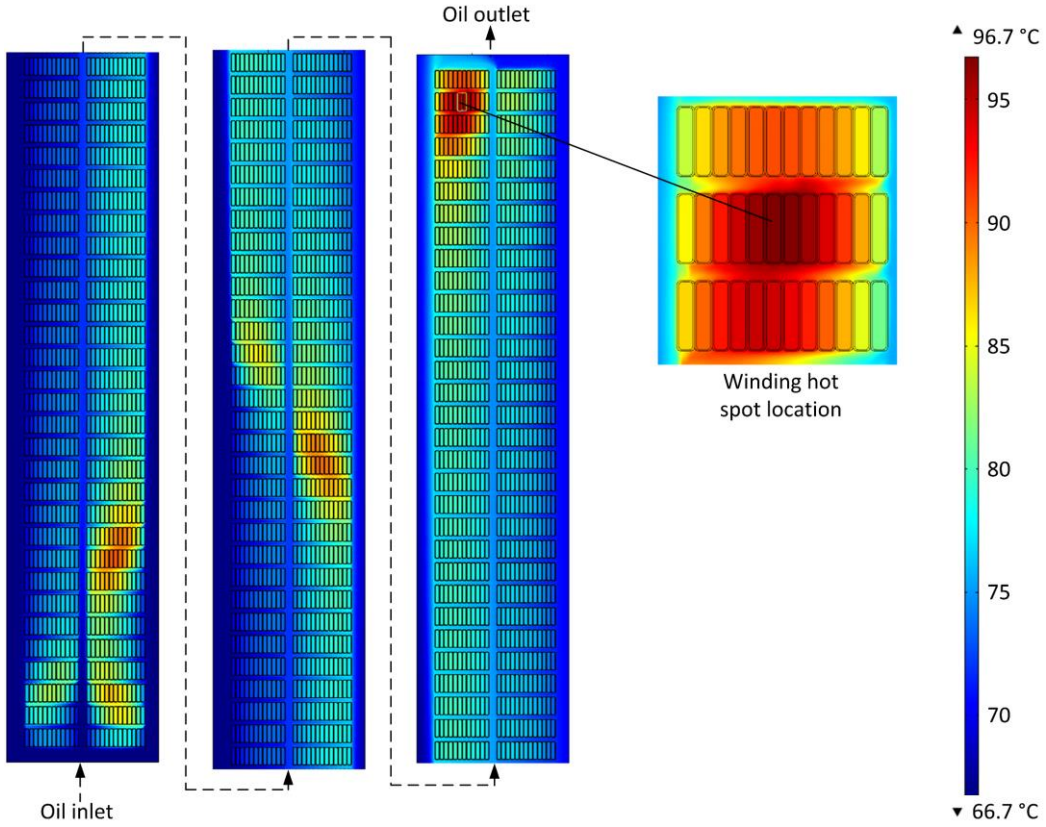

Fig. 7. Thermal distribution contour plot and hot-spot location

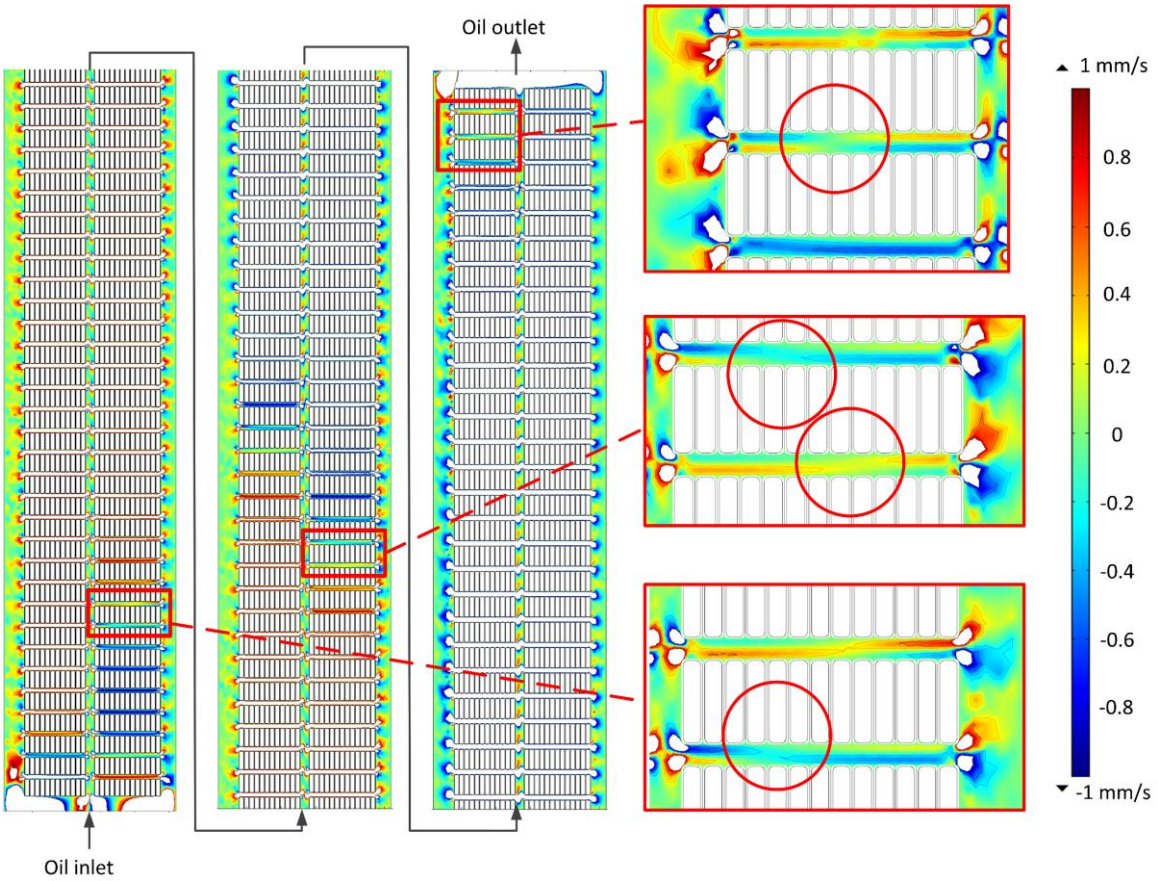

Fig. 8. Radial oil flow distribution with 'stagnant oil zone'

3.3 Maximum Temperature – Average Oil Flow Velocity (Radially) Plots

In this context, the complex structure of thermal distribution and oil flow scheme of oil natural cooled non-guided winding is presented in Figures 9 and 10. Figure 9 reveals the unpredictable maximum temperature profiles for both inner and outer disc winding. Both sections are showing a similar pattern with a temperature difference between 3ºC and 16ºC. Disc 93 of the inner disc showed a peak value of 96.7ºC, whilst 90.5ºC is the peak temperature noticed at disc 9 of the outer disc section.

Figure 10 demonstrates the average radial oil velocity in each radial cooling duct. Surprisingly, the oil flow formed a zigzagging pattern even without the existence of washer as in the GOF winding cooling design. The negative value of oil velocity means the oil flow to the left, on the other hand, positive oil flow shows otherwise. This zigzagging flow behaviour is mainly due to the unpredictable pressure gradient developed between two ends of duct oil. This pressure gradient exists by the uneven expansion of oil density at both duct-ends due to the rising in temperature as a result from the different rates of heat absorption from the copper strand and as well as by the size difference between vertical cooling ducts. As mentioned earlier in the winding geometry, the winding has 12 mm inner vertical oil duct and 9 mm outer vertical duct with 5 mm intermediate cooling duct which separated the disc into two sections. There was nearly no moving oil (stagnant of oil) at duct number 2, 10, 45 and 92.

Figures 11 and 12 describe the interrelation between oil flow velocity and disc temperature for both inner and outer disc sections. The red line in these figures is known as the zero-crossing line which represents the points where the oil flow changes its direction from left to right or vice versa.

It is shown that the oil flows near to the zero-crossing line reflects the higher temperature on the adjacent disc. These can be seen at oil duct numbers 1-2, 47-48 and 91-92 correspond to the disc temperature of 83ºC (disc no.3), 86ºC (disc no.50) and 96.7ºC (disc no.93) as shown in Figure 11. A similar pattern occurs at the outer segment of discs as shown in Figure 12.

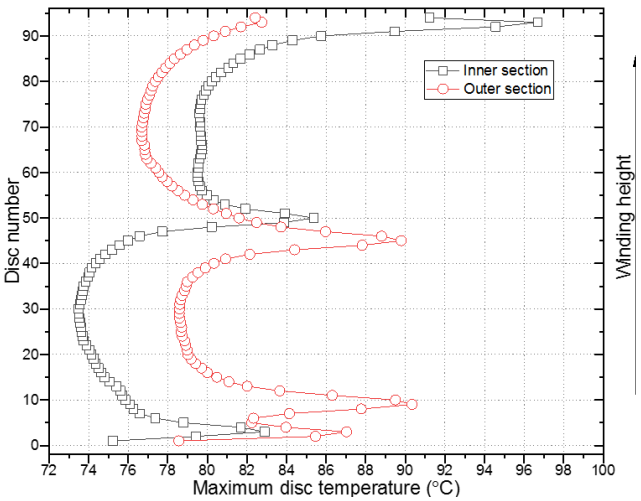

Fig. 9. Maximum disc temperature

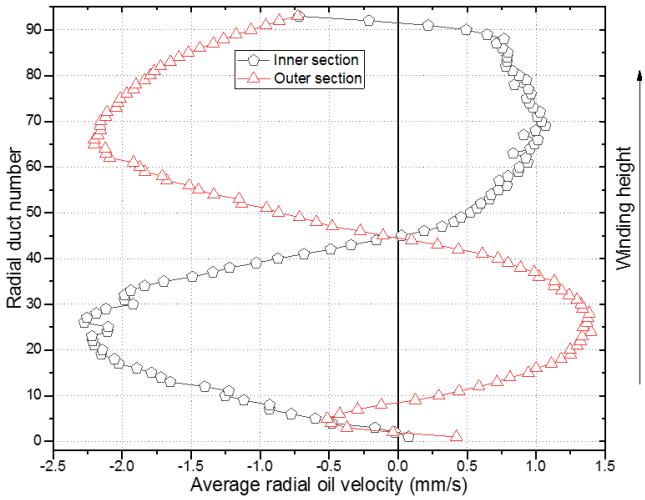

Fig. 10. Average radial oil flow velocity

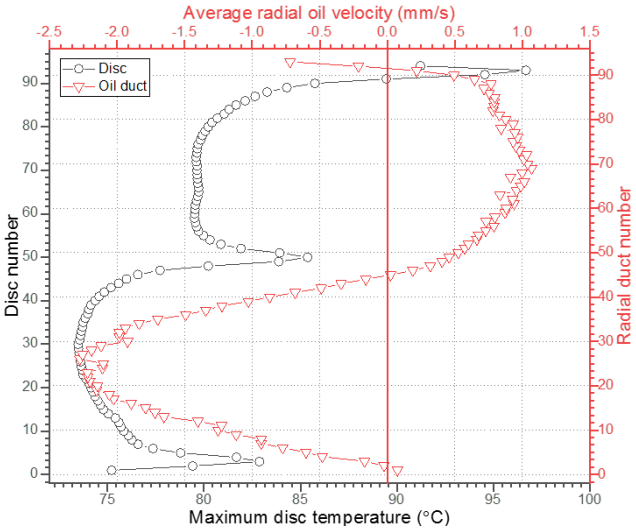

Fig. 11. Disc temperature – average radial oil flow (inner disc)

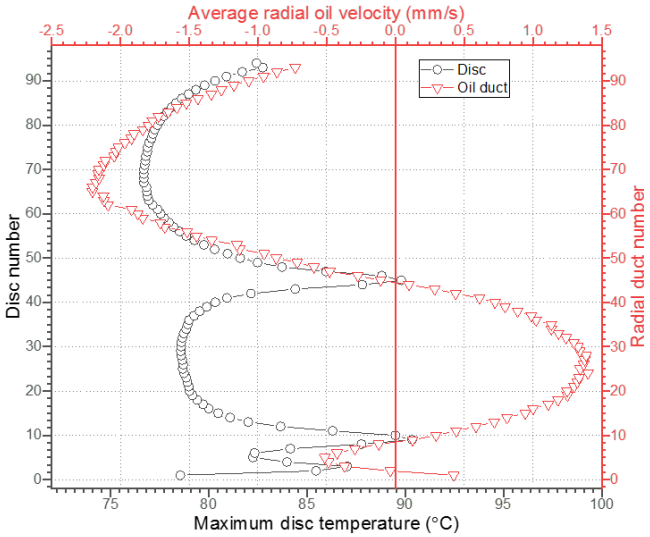

Fig. 12. Disc temperature – average radial oil flow (Outer disc)

4. Conclusions

2D CFD model provides an in-depth understanding of behavioural thermal and fluid flow distributions within the winding. The correlation between theses phenomenon proves that at low-velocity field oil duct region impacted on the rate of heat transfer from winding to the cooling medium. The mechanism of hot-spot region development can be well understood by the presented figures and it is purely hydrodynamic arguments. From the temperature distribution and the flow distribution figures, it is evident that these two physics are strongly coupled. For naturally cooled transformer winding by the convection of oil, the oil flow rate and its flow pattern are fully controlled by the buoyancy force due to the gravitational pull. As such, the unstructured oil flow pattern developed in the non-guided winding creates critical zones which leads to higher temperatures due to the occurrence of stagnant oil. The presented thermal plot demonstrates the hot-spot is not located at the top-most of disc winding. It has to be noted that in 2D approximation some components were unable to be modelled (axial spacer, vertical strip and cooling band). This disadvantage may cause errors in approximating the distributions of both fluid flow and thermal. The developed model can be used for further investigation, such as a parametric analysis on the winding geometry (vertical and horizontal oil ducts) in order to show how hot-spot temperature (location and value) relates to oil flow conditions. Besides, this model would also be a useful tool for thermal design optimisation by the transformer manufacturers.

Acknowledgment

The authors would like to thank Universiti Teknikal Malaysia Melaka (UTeM) and Universiti Putra Malaysia (UPM) for all the support.

References

[1] Kassi, K. S., I. Fofana, F. Meghnefi, and Z. Yeo. "Impact of local overheating on conventional and hybrid insulations for power transformers." *IEEE Transactions on Dielectrics and Electrical Insulation* 22, no. 5 (2015): 2543-2553. https://doi.org/10.1109/TDEI.2015.005065

[2] CIGRE Working Group A2.24. (2009). "Thermal Performance of Transformers."

[3] CIGRE Task Force D1.01.10. (2007). "Ageing of Celluose in Mineral-Oil Insulated Transformers."

[4] IEC, IEC. "60076-7, Loading Guide for Oil-Immersed Power Transformers." *Geneva, Switzerland: IEC* (2005).

[5] Board, I. "Ieee guide for loading mineral-oil immersed transformers." *IEEE Std C* 57 (1995): 1-112.

[6] Cigre Working Group A2.37. (2015). "Transformer Reliability Survey."
[7] Lecuna, Ramon, Fernando Delgado, Alfredo Ortiz, Pablo B. Castro, Inmaculada Fernandez, and Carlos J. Renedo. "Thermal-fluid characterization of alternative liquids of power transformers: A numerical approach." *IEEE Transactions on Dielectrics and Electrical Insulation* 22, no. 5 (2015): 2522-2529. https://doi.org/10.1109/TDEI.2015.004793
[8] Weinläder, A., W. Wu, S. Tenbohlen, and Z. Wang. "Prediction of the oil flow distribution in oil-immersed transformer windings by network modelling and computational fluid dynamics." *IET electric power applications* 6, no. 2 (2012): 82-90. https://doi.org/10.1049/iet-epa.2011.0122
[9] Mufuta, Jean-Michel. "Comparison of experimental values and numerical simulation on a set-up simulating the cross-section of a disc-type transformer." *International journal of thermal sciences* 38, no. 5 (1999): 424-435. https://doi.org/10.1016/S0035-3159(99)80031-2
[10] Paramane, Sachin B., Wim Van der Veken, Atul Sharma, and Joris Coddé. "Effects of oil leakage on thermal hydraulic characteristics and performance of a disc-type transformer winding." *Applied Thermal Engineering* 98 (2016): 1130-1139. https://doi.org/10.1016/j.applthermaleng.2015.12.141
[11] Ab Ghani, Sharin, Norazhar Abu Bakar, Imran Sutan Chairul, Mohd Shahril Ahmad Khiar, and Nur Hakimah Ab Aziz. "Effects of Moisture Content and Temperature on the Dielectric Strength of Transformer Insulating Oil." *Journal of Advanced Research in Fluid Mechanics and Thermal Sciences* 63, no. 1 (2019): 107–116.
[12] Torriano, F., M. Chaaban, and P. Picher. "Numerical study of parameters affecting the temperature distribution in a disc-type transformer winding." *Applied Thermal Engineering* 30, no. 14-15 (2010): 2034-2044. https://doi.org/10.1016/j.applthermaleng.2010.05.004
[13] Torriano, F., P. Picher, and M. Chaaban. "Numerical investigation of 3D flow and thermal effects in a disc-type transformer winding." *Applied Thermal Engineering* 40 (2012): 121-131. https://doi.org/10.1016/j.applthermaleng.2012.02.011
[14] El Wakil, N., N-C. Chereches, and J. Padet. "Numerical study of heat transfer and fluid flow in a power transformer." *International Journal of Thermal Sciences* 45, no. 6 (2006): 615-626. https://doi.org/10.1016/j.ijthermalsci.2005.09.002
[15] COMSOL. "Chapter 3: Single-Phase Flow Physics Interface." in *CFD Module User's Guide*, pp. 49–188, 2014.
[16] Wijaya, Jaury, Wenyu Guo, Tadeusz Czaszejko, Daniel Martin, Nick Lelekakis, and Dejan Susa. "Temperature distribution in a disc-type transformer winding." In *2012 7th IEEE Conference on Industrial Electronics and Applications (ICIEA)*, pp. 838-843. IEEE, 2012. https://doi.org/10.1109/ICIEA.2012.6360841
[17] Chereches, Nelu-Cristian, Monica Chereches, Livia Miron, and Sebastian Hudisteanu. "Numerical study of cooling solutions inside a power transformer." *Energy Procedia* 112 (2017): 314-321. https://doi.org/10.1016/j.egypro.2017.03.1103
[18] COMSOL. "Chapter 4: Heat Transfer and Non-Isothermal Flow Physics Interfaces. " In *CFD Module User's Guide*, pp. 188–288, 2014.
[19] Lienhard, John H. *A heat transfer textbook*. Courier Dover Publications, 2019.
[20] Zhang, Jiahui, and Xianguo Li. "Coolant flow distribution and pressure loss in ONAN transformer windings $ Part I: Theory and model development." *IEEE Transactions on Power Delivery* 19, no. 1 (2004): 186-193. https://doi.org/10.1109/TPWRD.2003.820225
[21] Skillen, Alex, Alistair Revell, Hector Iacovides, and Wei Wu. "Numerical prediction of local hot-spot phenomena in transformer windings." *Applied Thermal Engineering* 36 (2012): 96-105. https://doi.org/10.1016/j.applthermaleng.2011.11.054
[22] Kranenborg, E. J., C. O. Olsson, B. R. Samuelsson, L. Å. Lundin, and R. M. Missing. "Numerical study on mixed convection and thermal streaking in power transformer windings." In *Fifth European Thermal-Sciences Conf., The Netherlands*. 2008.
[23] COMSOL. "Chapter 2: Modeling and Simulations of fluid flows. " In *CFD Module User's Guide*, pp. 31–48, 2014.